Four dimensional mapping of tracer channelization in subhorizontal bedrock fractures using surface ground penetrating radar

Jennifer Talley, Gregory S. Baker, Matthew W. Becker, and Nicholas Beyrle
Geology Department, University at Buffalo, Buffalo, New York, USA

Received 11 November 2004; revised 31 December 2004; accepted 24 January 2005; published 22 February 2005.

[1] To observe flow channeling in situ, surface ground-penetrating radar (GPR) was used to detect a saline tracer moving through a sub-horizontal bedrock fracture. The tracer is mapped using amplitude variations resulting from the significant difference in electromagnetic properties between the tracer and natural ground water within the fracture. Results show that hydrogeophysical investigations using GPR can successfully image tracer movement in a variety of flow configurations in three spatial dimensions through time (hence 4D). Observed tracer travel paths demonstrated meter-scale spatial variability that may be attributed to heterogeneity in fracture aperture. **Citation:** Talley, J., G. S. Baker, M. W. Becker, and N. Beyrle (2005), Four dimensional mapping of tracer channelization in subhorizontal bedrock fractures using surface ground penetrating radar, *Geophys. Res. Lett.*, *32*, L04401, doi:10.1029/2004GL021974.

1. Introduction

[2] Laboratory and theoretical studies suggest ground water in fractured bedrock is focused along certain "paths of least resistance" related to the fracture aperture distribution [*Tsang and Neretnieks*, 1998]. Ground-water contaminants are likely to follow these pathways, making it difficult in practice to locate affected areas without detailed knowledge of channel location and geometry. This research tests whether surface GPR can be used to detect saline tracer in a sub-horizontal fracture and shows, for the first time, map view images of channelized fluid flow in bedrock. Although these techniques are practical only under very specific geological conditions, the results of these experiments yield images that provide a conceptual foundation for understanding fracture flow processes at the field scale.

2. Background

[3] Surface ground penetrating radar (GPR) is a non-invasive geophysical method that transmits electromagnetic waves into the subsurface where they scatter at interfaces with contrasting electrical properties and reflect back to the surface. The depth to a reflector may be determined through wave arrival times if the electromagnetic velocity of the geologic material is known. Recent investigations [e.g., *Baker*, 1998; *Jordan et al.*, 2004] have demonstrated the usefulness of GPR in hydrogeophysical studies through examination of small variations in signal attributes such as amplitude. Additionally, *Tsoflias et al.* [2001] mapped fluid drainage during a pumping test based on amplitude differences between saturated and air-filled dissolution features, and other researchers have used cross-borehole GPR surveys involving saline tracer to locate fracture flow through attenuation difference tomography [e.g., *Lane et al.*, 1998; *Day-Lewis et al.*, 2003]. The work presented here differs from these previous field studies because it shows spatial variations in fluid flow that provide a basis for investigating the spatial correlation structure of aperture. A measurement of aperture distribution in the fracture plane is essential to understanding the manner in which fluid velocity and solute dispersion are affected by the spatial correlation of fracture apertures.

[4] First, it was established that variations in fluid conductivity within a saturated variable aperture fracture could be detected by GPR to test the theoretical basis of the experiments. This was completed by creating an analytic model for reflections from a fluid-filled horizontal fracture based on fundamental radar equations and the electrical characteristics of the subsurface at the experiment site obtained from preliminary common mid point GPR data.

[5] A propagating wave reflects from a horizontal interface dividing two layers with contrasting electrical properties according to

$$R_{12} = \left(k_1^{1/2} - k_2^{1/2}\right)\left(k_1^{1/2} + k_2^{1/2}\right)^{-1} \tag{1}$$

for the simplified normal incidence case where k_1 and k_2 represent the wave numbers of medium 1 and 2. Wave number is related to electrical properties of the subsurface by

$$k = \omega v^{-1} + i\alpha \tag{2}$$

$$\alpha = 0.5\sigma\left(\mu\varepsilon^{-1}\right)^{1/2} \tag{3}$$

where ω is the angular frequency, v is the phase velocity, μ is the magnetic permeability, ε is the dielectric permittivity, and σ is the electrical conductivity.

[6] For a thin horizontal layer (e.g., a fluid-filled planar fracture) the reflection coefficient is influenced by constructive and destructive interference from the multiple reflections that cause a time delay and phase shift of the resulting signal. The reflection coefficient of a thin layer in this setting is given by *Hollender and Tillard* [1998]:

$$R(\omega) = R_{12} + T_{12}T_{21}\Sigma R_{21}^{(2n-1)} \exp(-in2dk_2 \cos\theta_t) \tag{4}$$

In equation (4), R_{12} and T_{12} are the Fresnel reflection and transmission coefficients at the boundary between media 1 and 2, d is the layer thickness, and θ_t is the refraction angle.

0094-8276/05/2004GL021974$05.00

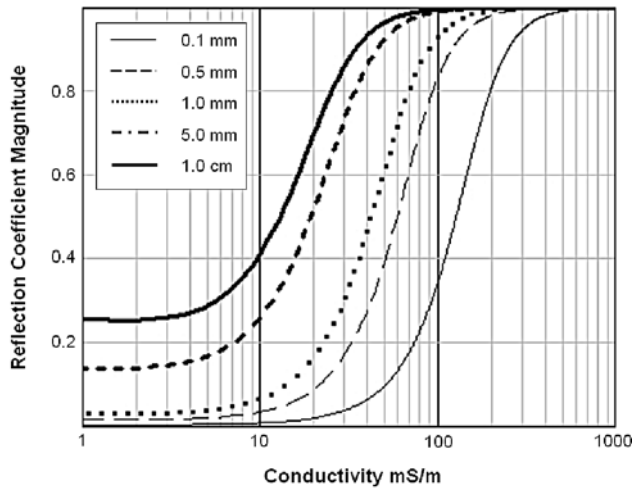

Figure 1. Reflectivity variations with conductivity and fracture aperture at 100 MHz for the EV case.

[7] Analytic modeling of reflections from a thin layer having varying conductivity based on these equations shows that, in general, as the layer thickness and conductivity increase the reflection coefficient increases as well. Figure 1 demonstrates this relationship for electrical properties specific to the experiment site, where the wave velocity is 0.11 m/ns and the relative dielectric permittivities of the rock matrix and water within the fracture are constant at 7 and 80, respectively. In this example, reflection coefficient magnitudes were calculated for the EV (also called TM) case where the incident electric field is polarized parallel to the incidence plane for a wave propagating through a uniform rock matrix (v = 0.11 m/ns, σ = 0.1 mS/m) that is reflected at a horizontal fracture of aperture d filled with water of conductivity σ. Additional assumptions are that $\theta_i = 0$ and the magnetic permeabilities of layers 1 and 2 are equal to that of free space, μ_0. The model results shown in Figure 1 predict that radar reflection amplitudes for this particular example with all other electrical properties constant should be sensitive to changes in electrical conductivity between 10 and 100 mS/m (NaCl concentration between 180 and 1800 mg/L). The surface GPR tracer experiments were designed specifically for this site based on these model results of reflection variations resulting from changing the electrical conductivity of fluid within a variable aperture horizontal fracture.

3. Test Site Description

[8] Field experiments were performed near Chasm Lake at the Altona Flat Rock Site, located approximately 15 km northwest of Plattsburgh, New York, USA (Figure 2). Flat Rock is part of a system of Cambrian Potsdam Sandstone pavements that were stripped of overburden during the last glaciation and remain exposed today. The Potsdam in the test area is well-sorted, highly lithified quartzose sandstone. There are two orthogonal vertical fracture sets at the site oriented roughly N-S and E-W, as well as laterally extensive sub-horizontal (dipping <3°) bedding plane partitions that are visible in numerous vertical outcrops surrounding the site. Hydraulic tests show that some sub-horizontal fractures provide an effective secondary porosity that is significantly larger than the primary porosity of the rock matrix (<10%). The channeling experiments described here were conducted in a series of 15-cm-diameter wells arranged in a 5-spot configuration (Figure 3) having 10 meters on a side that each intersect a major sub-horizontal fracture 7.6 meters below ground surface. Results of hydraulic testing indicate that all five wells communicate via this relatively shallow fracture with an approximate transmissivity of 5 m^2/day, which suggests a mean aperture of 0.45 mm [*Becker and Shapiro*, 2003]. The combination of hydraulic connectivity between wells, simplicity of the fracture system, and good GPR conditions (e.g., no overburden and low background electrical conductivity) make this site ideal for tracer-mapping experiments using GPR.

4. Data Collection and Analysis

[9] Saline tracer GPR tests were conducted in various flow configurations to determine how flow channels develop under different hydraulic conditions. A natural gradient test was conducted first by adding NaCl into one well (204) and tracking the saline plume as it moved down gradient. Prior to introduction of NaCl, an inflatable PVC packer was installed in well 204 at a depth of 8.2 m to isolate the fracture above the packer. A set of six 100 MHz, EV polarized (Figure 4), 10-cm step GPR lines were collected orthogonal to the natural flow direction during a 30-minute period with PulseEKKO 100A GPR equipment to determine background conditions. After adding 3 kg NaCl(s) and continuously mixing the borehole, two more sets of GPR data were collected starting 1 and 2 hours after introduction of the NaCl (each set took approximately 30 minutes). Electrical conductivity was measured in nearby wells throughout the experiment to determine tracer concentrations and ensure that all NaCl was removed from the system after the test.

[10] Forced gradient fluid injection ''dipole'' tracer experiments were conducted in two directions: between 204 and 304 and between 104 and 504. For the first experiment, inflatable PVC packers were installed in the injection (204) and pumping (304) wells at respective

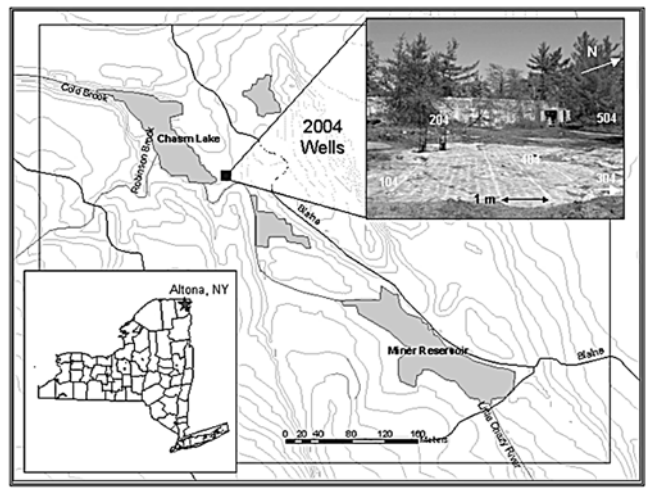

Figure 2. Altona Flat Rock site map.

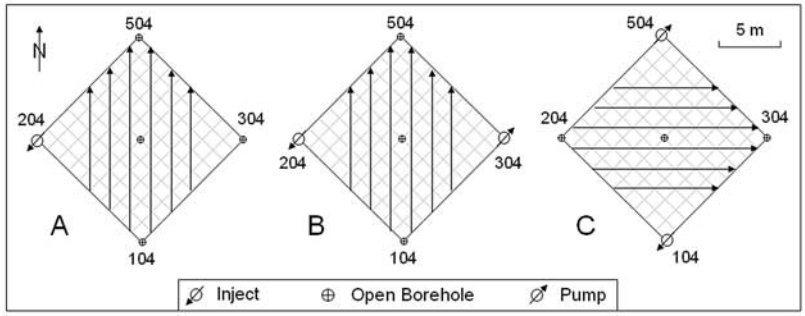

Figure 3. Well configuration and GPR survey lines for A) natural gradient test, B) dipole I test, and C) dipole II test.

depths of 8.2 and 8.0 m. Fluid dipole flow (12.4 L/min) was established by lowering the outlet hose from 304 into 204 and allowing flow to circulate between the two wells. The same GPR profiles collected during the natural gradient test were collected prior to injection with the dipole system at steady-state (without NaCl) to obtain background information. Shortly after 3 kg NaCl were added and mixed in 204, another set of GPR profiles were collected. Electrical conductivity was measured in the effluent from the pumping well to ensure that saline solution continued circulating through the system at relatively high dipole flow rates. The effluent hose was then removed from 204 and a final set of GPR profiles were collected as the saline fluid was pumped from the formation. For the second dipole test, PVC packers were installed in the injection (104) and pumping (504) wells at 7.9 m depth and dipole flow was established at a constant rate of 4.0 L/min. Two background sets of six GPR profiles (orthogonal to lines for the first dipole test) were collected prior to adding NaCl to well 104. After injecting 20 L of saturated NaCl solution through a reservoir into 104, three more sets of GPR profiles were collected starting 10 minutes, 1 hour, and 2 hours post-injection in the full dipole configuration. Figure 3 shows the well configuration and GPR layout for the natural gradient and fluid injection dipole tests.

[11] The GPR data were preprocessed using pulseEKKO software by applying DC shifts and low-frequency noise corrections and adjusting data to the proper zero time, then imported into seismic processing and imaging software (Kingdom Suite +) and further processed using a low-pass 120 MHz filter to remove high frequency noise. The low-pass filter improved data quality while preserving relative amplitude information at the horizon of interest. The amplitudes at the reflector corresponding to the sub-horizontal fracture ($\sim$140 ns) were isolated by selecting horizons at the top and bottom of the first positive peak in the reflector and integrating between the two horizons to characterize the entire waveform peak for each trace. The integrated amplitudes from the reflector of interest were then normalized to the integrated amplitude of the airwave to remove trace by trace gain effects.

[12] The normalized amplitudes were used to create a map of the fracture for each background and post-tracer GPR dataset for all three tests. Amplitudes between lines were interpolated with a simple kriging scheme to provide a continuous surface bounded by the first and last lines of each set. The two background sets for the second dipole test were compared to determine the expected degree of natural variability for GPR runs with the same layout. The background set for each test was then subtracted from each successive post-tracer set from the same test to show where reflection amplitudes increased due to presence of the tracer. Although each subtraction map represents reflection variations at a given time after injection, it is important to note that changes in tracer location and concentration during collection of each GPR set may result in discontinuities between lines due to the dynamic nature of these experiments.

5. Results

[13] The two background GPR line sets for the second dipole test are comparable, showing good data repeatability under the same conditions with a standard normalized amplitude deviation of 0.001 (Figure 5). This suggests that major amplitude changes between background and post-tracer sets are related to the presence of saline tracer in the fracture. Figure 6 shows map-view images of amplitude changes through time at the target fracture for each test. In all three cases it is clear that the saline tracer developed channeled flow features in the fracture, and in general these channeled patterns varied under different hydraulic conditions. The largest and most continuous amplitude increases are visible in the natural gradient test, where the electrical conductivity measured one hour after injection in well 404 in the center of the grid (2640 mS/m) was three orders of magnitude larger than the background conductivity.

Figure 4. EV GPR polarization with long axis of antennae in line with survey.

Similar patterns are visible for the dipole tests, but amplitude changes are generally less dramatic than the natural gradient test because of additional dilution introduced by the dipole flow configuration. Electrical conductivities measured continuously at the re-injection point for each dipole test ranged from around 10 to 1000 mS/m, indicating that the saline solution conductivity within the fracture is sufficient to increase GPR reflections as predicted by the analytic model results. However, within the tracer plume there is believed to be little amplitude variation because—as the theoretical predictions indicate—reflection coefficients are maximized at conductivities above 300 mS/m (~5400 mg/L NaCl) for an average aperture of 0.5 mm. The field experiment results correlate well qualitatively to the model results since reflection increases related to fluid electrical conductivity variations in the 10 to 1000 mS/m range are observed as predicted by the analytic model. Work is currently under way to make a more quantitative comparison of model and field results using controlled lab measurements.

6. Conclusions

[14] Surface ground-penetrating radar was successfully used for 4D (time-lapse, map-view) imaging of saline tracer moving through a sub-horizontal fracture plane in different flow configurations. Background data were subtracted from post-tracer injection data to show amplitude increases caused by the conductive tracer moving through the fracture. Tracer movement was confirmed with electrical conductivity measurements taken in wells along the direction of flow. These results concur with theoretical understanding of radar energy reflection from thin subsurface layers with known electrical properties. Tracer migration paths shown in GPR images exhibit meter-scale spatial variability that can be attributed to channelized ground-water flow. Work is under way to refine these methods to the point where aperture variability within a single fracture is inferred from GPR amplitude returns, as well as to perform a direct quantitative comparison of model and field results. Careful integration of hydraulic, tracer, and GPR techniques will yield a better understanding of the complex nature of ground-water flow through fractured bedrock.

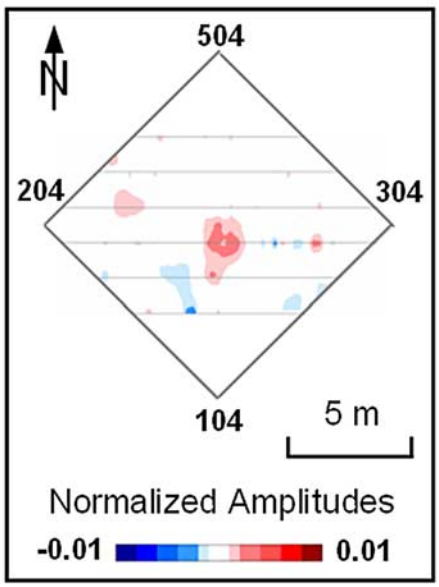

Figure 5. Map view of difference between two background GPR sets for dipole II test.

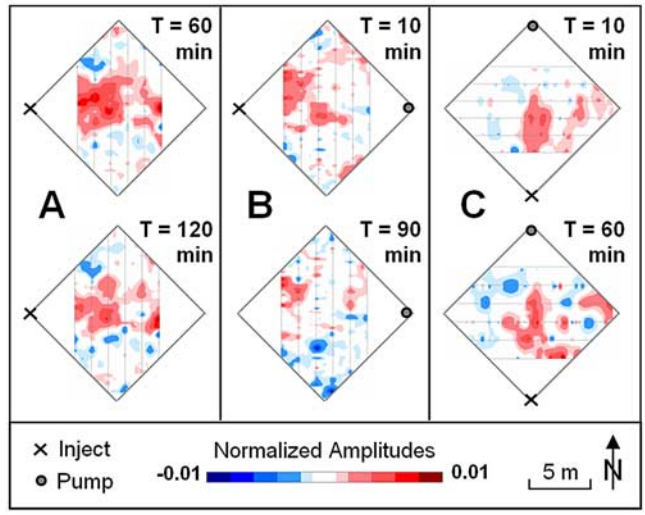

Figure 6. Map view of background subtracted from post-tracer runs at different times after injection for A) natural gradient test, B) dipole I test, and C) dipole II test.

[15] **Acknowledgments.** This research is partially supported through National Science Foundation Grant GEO-0207720. Kingdom Suite + data analysis software was provided through an educational grant by Seismic Micro-Technology, Inc. The authors would also like to thank Fred Paillet, David Franzi, Edwin Romanowicz, the William H. Miner Agricultural Institute, and two anonymous reviewers.

References

Baker, G. S. (1998), Applying AVO analysis to GPR data, *Geophys. Res. Lett.*, *25*(3), 397–400.

Becker, M. W., and A. M. Shapiro (2003), Interpreting tracer breakthrough tailing from different forced-gradient tracer experiment configurations in fractured bedrock, *Water Resour. Res.*, *39*(1), 1024, doi:10.1029/2001WR001190.

Day-Lewis, F. D., J. W. Lane Jr., J. M. Harris, and S. M. Gorelick (2003), Time-lapse imaging of saline-tracer transport in fractured rock using difference-attenuation radar tomography, *Water Resour. Res.*, *39*(10), 1290, doi:10.1029/2002WR001722.

Hollender, F., and S. Tillard (1998), Modeling ground-penetrating radar wave propagation and reflection with the Jonscher parameterization, *Geophysics*, *63*(3), 1933–1942.

Jordan, T. E., G. S. Baker, K. Henn, and J. P. Messier (2004), Using amplitude variation with offset and normalized residual polarization analysis of ground penetrating radar data to differentiate an NAPL release from stratigraphic changes, *Journal of Applied Geophysics*, *56*(1), 41–58.

Lane, J. W., Jr., P. K. Joesten, F. P. Haeni, M. Vendl, and D. Yeskis (1998), Use of borehole-radar methods to monitor the movement of saline tracer in carbonate rock at Belvidere, Illinois, paper presented at Symposium on the Application of Geophysics to Engineering and Environmental Problems, Environ. and Eng. Geophys. Soc., Chicago, Ill.

Tsang, C. F., and I. Neretnieks (1998), Flow channeling in heterogeneous fractured rocks, *Rev. Geophys.*, *36*(2), 275–298.

Tsoflias, G. P., T. Halihan, and J. M. Sharp Jr. (2001), Monitoring pumping test response in a fractured aquifer using ground-penetrating radar, *Water Resour. Res.*, *37*(5), 1221–1229.

G. S. Baker, M. W. Becker, N. Beyrle, and J. Talley, Geology Department, University at Buffalo North Campus, 876 Natural Sciences Complex, Amherst, NY 14261, USA. (jltalley@buffalo.edu)